Paper No.
67—WA/FE-9

R. MANI[1]

A. J. ACOSTA
Mem. ASME
Division of Engineering and Applied Science,
California Institute of Technology,
Pasadena, Calif.

Quasi Two-Dimensional Flows Through a Cascade

A thin airfoil theory is developed for airfoils spanning a slowly diverging or converging channel, the motivation being to predict, theoretically, the effect of varying axial velocity on the cascade performance of axial flow compressor rows.

Introduction

THERE are two problems to be solved in axial flow turbomachine aerodynamics. The first, the so-called "through-flow" problem, studies the average flow in a meridional plane. The second, the cascade problem, studies the flow past a finite number of blades cut by the rotational stream surfaces. In the first problem, one usually assumes axisymmetry corresponding physically to having an infinite number of blades. In the second problem, it is usual to ignore the radial velocities so that the flow in one rotational stream surface is uncoupled from the flow in adjacent stream surfaces.

The direct cascade problem consists of predicting the forces on the blades given in advance the axisymmetric flow through them. If one assumes the axisymmetric surfaces to be parallel to one another with the gap between them constant, then by suitable mapping the cascade problem is reduced to a two-dimensional problem in a plane. Assuming no vorticity normal to this plane and an incompressible fluid leads to a boundary value problem with the two-dimensional potential equation as the governing equation. In this plane there are an infinite number of identical airfoils subject to a given upstream velocity.

Actually, however, both due to deliberate design and the growth of boundary layers on the bounding walls, the adjacent stream surfaces are not parallel. The gap between them varies with axial location and is usually decreasing in the downstream direction. The present work examines theoretically the effect of this contraction of the stream surfaces on the performance of the airfoils spanning them.

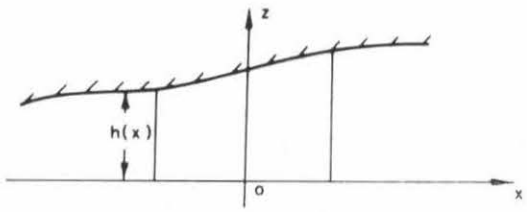

Fig. 1 Definition sketch for class of flows considered

Class of Flows to Be Considered

The flow is assumed to be inviscid, irrotational, and incompressible. Thus it is describable in terms of a velocity potential ϕ which satisfies:

$$\nabla^2\phi = 0 \tag{1}$$

It is assumed to be taking place in a channel as in Fig. 1 whose height h is only a function of x. The channel represents the developed form of the annular portion between two adjacent stream surfaces of a turbomachine. The assumed independence of h with y then corresponds to assuming axisymmetry of the stream surfaces of revolution in a machine or its counterpart found in experimental tests of cascades.

A key assumption in the work to follow is that $h(x)$ is a slowly varying function of x. It is clear that if $h(x)$ were constant, the flow in the channel would be two-dimensional. If $h(x)$ is a slowly varying function of x, the departure of the flow in the channel

[1] Now, Fluids Mechanics Engineer, General Electric Research and Development Center, Schenectady, N. Y.

Contributed by the Fluids Engineering Division for presentation at the Winter Annual Meeting, Pittsburgh, Pa., November 12–17, 1967, of THE AMERICAN SOCIETY OF MECHANICAL ENGINEERS. Manuscript received at ASME Headquarters, August 1, 1967. Paper No. 67—WA/FE-9.

Nomenclature

Δb = width of streamtube (Fig. 2)
c = chord
Cb = lift coefficient of an isolated circular arc airfoil at zero angle of attack
h = height of channel
i = $\sqrt{-1}$
k = transform variable
K = kernel function
K_0 = modified Bessel Function of second kind of order zero
m = source density
r = $\sqrt{x^2 + y^2}$
s = spacing
t/c = thickness ratio
u, v, and w = x, y, and z-components of velocity
V = freestream velocity
x, y, and z = Cartesian coordinates
α = contraction parameter
δ = angle which the vector mean velocity makes with the blade chord at the midpoint of blade chord
Δ = $\dfrac{\partial^2}{\partial x^2} + \dfrac{\partial^2}{\partial y^2}$
∇^2 = $\dfrac{\partial^2}{\partial x^2} + \dfrac{\partial^2}{\partial y^2} + \dfrac{\partial^2}{\partial z^2}$
γ = vortex density
Γ = total circulation
ϕ = velocity potential; also transformed chord coordinate
λ = stagger angle; also angle between blade chord and axis of convergence
ψ = stream function
θ = polar angle coordinate; also transformed chord coordinate

Subscripts

c = cascade
cb = camber
l = lower
m = mean
n = normal
0 = at the origin
r = regular
s = source
t = tangential
th = thickness
v = vortex
x, y, and z — denotes partial differentiation with respect to that variable

Superscripts

$\overline{\ \ }$—denotes average over gap
$'$—denotes $\left(\dfrac{d}{dx}\right)$

Discussion on this paper will be accepted at ASME Headquarters until December 18, 1967

from a strict two-dimensional one is small—hence the use of the phrase "quasi two-dimensional" to describe such a flow.

The Averaged Equations

We anticipate that the flow will be nearly two-dimensional for the reasons mentioned above and that as a consequence, the velocity vector will lie mainly in the x-y plane. There will still be small velocity variations across the height of the passage as equation (1) is essentially three-dimensional. But as they are expected to be small, it should be possible to use values across the passage with little error, and as a result, a two-dimensional equation is obtained. Averages across the gap height are defined as below:

$$\bar{\phi} = \frac{1}{h}\int_0^h \phi dz, \qquad \bar{u} = \frac{1}{h}\int_0^h u dz, \text{ etc.} \tag{2}$$

It is also convenient to average the continuity equation and the z-component of irrotationality requirement. These equations are

$$u_x + v_y + w_z = 0 \tag{3}$$

$$v_x - u_y = 0, \tag{4}$$

respectively. Averages of these over the channel height are now formed as in equation (2). With the use of the kinematic boundary condition that $w(x, y, h) = h'u(x, y, h)$ they become

$$\frac{\partial}{\partial x}(h\bar{u}) + \frac{\partial}{\partial y}(h\bar{v}) = 0 \tag{5}$$

and

$$\frac{\partial \bar{v}}{\partial x} - \frac{\partial \bar{u}}{\partial y} = 0 \tag{6}$$

The first is exact and the latter is only approximate.

To the order of approximation used in the above we may equate $\bar{u}$ with $\bar{\phi}_x$ and $\bar{v}$ with $\bar{\phi}_y$. Then equation (5) gives for $\bar{\phi}$ the equation:

$$\Delta\bar{\phi} + \frac{h'}{h}\bar{\phi}_x = 0 \tag{7}$$

and letting $h\bar{u} = \bar{\psi}_y$ and $h\bar{v} = -\bar{\psi}_x$, equation (6) gives for $\bar{\psi}$ the equation:

$$\Delta\bar{\psi} - \frac{h'}{h}\bar{\psi}_x = 0 \tag{8}$$

Henceforth, because we deal exclusively with average quantities, bars will be dropped. The errors involved in the approximations used in deriving equations (6) and (7) have been discussed in reference [1].[1] We should also add that to the same order of approximation involved in deriving equation (7) and (8), the centerplane potential $\phi(x, y, 0)$ also satisfies:

$$\Delta\phi(x, y, 0) + \frac{h'}{h}\phi_x(x, y, 0) = 0.$$

There are two situations to which equations (7) and (8) may be applied. First, they could be used to study the flow in a channel of finite height as in Fig. 1. Then the equations apply in an approximate sense in that certain terms have been neglected. On the other hand, they could be applied to the developed form of an annular streamtube of infinitesimal width Δb as shown in Fig. 2. The flow in this annulus is exactly described by equations (7) and (8) in the limit as the width of the tube shrinks to zero. This would correspond to the channel of Fig. 1 when $h(x)$ and $h'(x)$ tend to zero, but $h'(x)/h(x)$ tends to some function of x.

[1] Numbers in brackets designate References at end of paper.

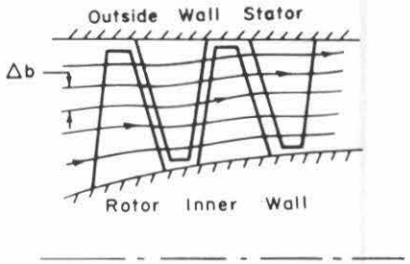

Fig. 2 Meridional section of an axial flow turbomachine

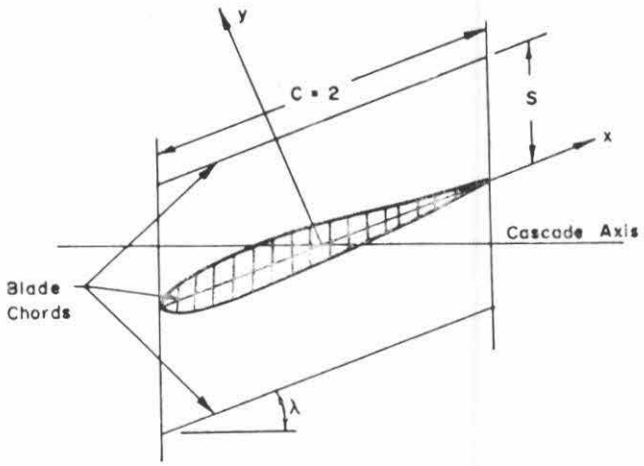

Fig. 3 Cascade nomenclature

In the application to the stream surfaces of Fig. 2, the only conditions needed to derive equations (7) and (8) are that continuity be satisfied and that the free vorticity normal to the stream surfaces be zero (which holds for a perfect fluid). The shed vorticity, if any, then enters only implicitly in the determination of the stream surfaces and hence it determines $h'(x)/h(x)$.

Types of Problems to Be Solved and Methods of Solution Used

We will be interested in situations in which the basic flow in the channel is perturbed by an airfoil or a cascade of airfoils. It is known that in plane cascade flows, this basic flow is the vector mean of the up-and-downstream velocity vectors across the cascade [2]. A similar mean velocity is also the basic flow even when the axial velocity is not constant [3]. In the present work we will be concerned with isolated airfoils and airfoils in cascade as sketched in Fig. 3. The airfoils perturb the basic flow whose magnitude at the center point of the chord is V_m and whose direction is inclined at the angle δ to the chord at this point. Because of the channel convergence, the speed of the basic flow varies unlike that of a plane flow. The angle between the axis of convergence and the chord, denoted by λ in Fig. 3, is the stagger angle of the cascade. The problem is now that of predicting the flow induced by a given cascade of airfoils having a known basic flow and channel convergence.

The approach to the problem and method of solution are modelled on that of [2]. In this, the "thin airfoil" approximation is used with the flow tangency condition being approximately satisfied on the chord rather than on the surface of the airfoil itself. Again, as in [2], the method of distributing singularities along the chord will be used. Thus a distribution of sources and vortex is laid out on the blade chords as in Fig. 4 in such a way that the flow is, approximately, tangential to blade surface.

Unlike the plane flow treatment of [2], however, the singular

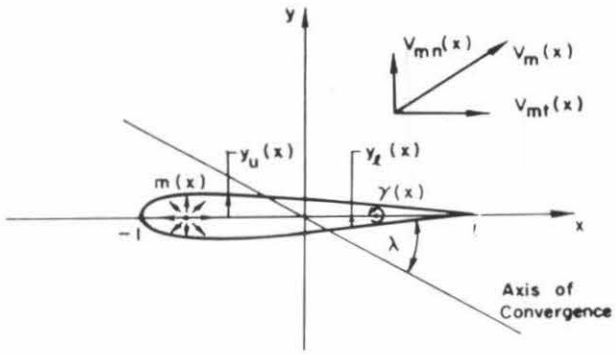

Fig. 4 Airfoil nomenclature

solutions corresponding to sources and vortex are now not known; they appear as the fundamental solutions of equations (7) and (8) and depend on the particular form of the channel used.

Boundary Conditions

As in thin airfoil theory, the airfoil is taken to consist of a thickness function $y_{th} = {}^1/_2(y_u - y_l)$ and a camber function $y_{cb} = {}^1/_2(y_u + y_l)$ where y_u and y_l are the upper and lower ordinates of the airfoil (Fig. 4). In the thin airfoil approximation, the source strength is given by

$$m(x) = 2V_{mt}\frac{dy_{th}}{dx} \tag{9}$$

where V_{mt} is the tangential component of the mean velocity. The tangency condition for the camber function is

$$\frac{dy_{cb}}{dx} = \frac{V_n}{V_t} \tag{10}$$

where V_n is the velocity normal to the chord and V_t is that tangential to the chord. These velocities have components from the mean velocities and also from the airfoils themselves. These latter contributions are symbolically expressed in the form of kernels $K_{snc}(x, \xi)$, $K_{stc}(x, \xi)$, $K_{vnc}(x, \xi)$ and $K_{vtc}(x, \xi)$. In these s and v denote "source" and "vortex," n and t denote normal and tangential to the chord, and c stands for "cascade." The meaning of the kernel function $K_{snc}(x, \xi)/2\pi$, for example, is that it is the normal velocity at point x of an airfoil in an infinite cascade due to a source of unit strength at points ξ on all airfoils of the cascade. The flow is periodic in the cascade so that the same source and velocity are found at corresponding points on all blades of the cascade, e.g., at points $S_{-\infty}, \ldots S_{-2}, S_{-1}, S_0, S_1 \ldots$. as indicated in Fig. 5. With these definitions, the flow tangency condition for the camber function is

$$V_{mn}(x) + \frac{1}{2\pi}\int_{-1}^{1}\{m(\xi)K_{snc}(x, \xi) + \gamma(\xi)K_{vnc}(x, \xi)\}d\xi = \frac{dy_{cb}}{dx}\left[V_{mt}(x) + \frac{1}{2\pi}\int_{-1}^{1}\{m(\xi)K_{stc}(\xi) + \gamma(\xi)K_{vtc}(x, \xi)\}d\xi\right] \tag{11}$$

where $m(x)$ is the known source distribution and $\gamma(x)$ is the unknown vorticity distribution.

Before proceeding to solve equation (1) we will outline the method used to obtain the source and vortex solutions for various types of channels.

Fundamental Source and Vortex Type Solutions

By a fundamental source type solution is meant the most elementary singular solution to equation (7). For example, the velocity potential for a source should become logarithmically singular at the origin.

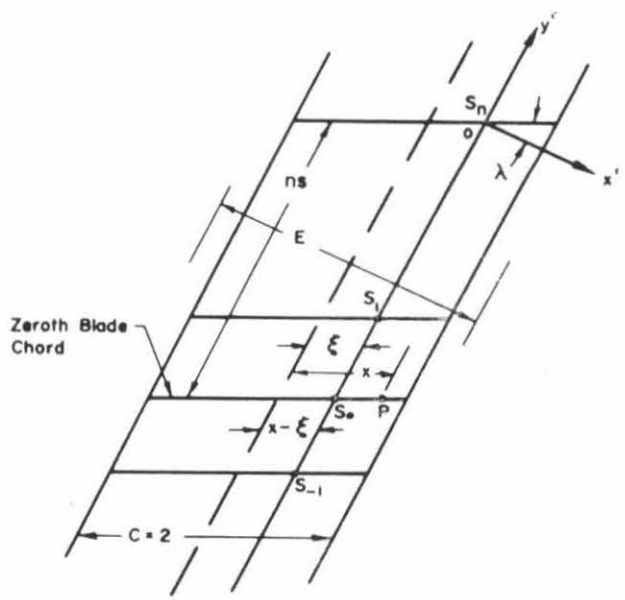

Fig. 5 Definition sketch for kernels

As an illustration consider the case of an exponentially converging channel, with $h = h_0 \exp(-\alpha x)$. Then equation (7) becomes

$$\Delta\phi = \alpha\phi_x.$$

The source type solution to this equation is

$$\phi = -\frac{1}{2\pi}\exp\left(\frac{\alpha x}{2}\right)K_0\left(\frac{\alpha r}{2}\right)$$

where $r = \sqrt{x^2 + y^2}$. A similar elementary singular solution for the stream function gives the velocity field for a vortex.

The finding of fundamental solutions for the above exponentially converging channel is quite easy and involves only an elementary transformation and separation of variables. Such a channel is, however, physically unrealistic because it flares to an infinite width far upstream and contracts to zero width far downstream. With a view to clarifying the effects of contraction for more realistic channels, efforts were made to find the solutions for fundamental sources and vortexes for channels in which (h'/h) differs from zero only over a finite extent of the x-axis. Outside of this region, the flow is two-dimensional. The procedure adopted is that described by Lighthill [4] and is based upon the use of Fourier exponential transforms. The use of Fourier exponential transforms to reduce a partial differential equation to an ordinary differential equation requires that the dependent variable vanish for large arguments. Since the potentials and stream functions do not possess this property, the problem has to be formulated in terms of velocities themselves.

As an illustration the procedure of calculating the v-component of velocity due to an isolated vortex of unit strength located at the origin in the x-y plane where the channel height is h_0 will be outlined following [4]. Since the field is completely free of sources, the averaged continuity equation is just equation (5). The averaged irrotationality condition [(equation 6)] is now written as

$$\frac{\partial}{\partial x}(hv) - \frac{\partial}{\partial y}(hu) - h'v = h_0\delta(x)\delta(y) \tag{12}$$

The product "$h_0\delta(x)\delta(y)$" on the right hand side of equation (12) represents the line vortex of strength h_0, and δ is the Dirac delta function. Eliminating (hu) leads to

$$\Delta v + \frac{h'}{h} v_x = \frac{h_0}{h(x)} \delta'(x)\delta(y) \tag{13}$$

The equation is transformed to standard form by the substitution

$$v = h_0^{1/2} h(x)^{-1/2} v_0$$

Then

$$\Delta v_0 - \left(\frac{1}{4}\left(\frac{h'}{h}\right)^2 + \frac{1}{2}\left(\frac{h'}{h}\right)'\right) v_0 = h_0^{1/2} h(x)^{-1/2} \delta'(x)\delta(y) \tag{14}$$

We now introduce the exponential transform in the usual way

$$p(x, k) = \frac{1}{2\pi} \int_{-\infty}^{\infty} \exp(iky) v_0(x, y) dy$$

so that

$$v_0 = \int_{-\infty}^{\infty} \exp(-iky) p(x, k) dk.$$

If we let $g(x) = \frac{1}{4}\left(\frac{h'}{h}\right)^2 + \frac{1}{2}\left(\frac{h'}{h}\right)'$ and apply the integral operator above, equation (14) reduces to

$$p'' - p(k^2 + g(x)) = \frac{1}{2\pi}\left[\delta'(x) + \frac{h'(0)}{2h(0)} \delta(x)\right]$$

It is assumed that both v_0 and its y derivative vanish for large y.

We have p satisfying

$$p'' - (g(x) + k^2)p = 0, \qquad x \neq 0 \tag{15}$$

and the jump conditions

$$p\Big|_{0-}^{0+} = \frac{1}{2\pi} \quad \text{and} \quad p'\Big|_{0-}^{0+} = \frac{1}{4\pi} \frac{h'(0)}{h(0)} \tag{16}$$

It is very difficult to determine the fundamental singular solutions from the formulation in equations (15) and (16). The solution of the ordinary differential equation (15) with conditions of equations of equation (16) is in itself not too difficult but the subsequent inversion of $p(x, k)$ to obtain $v_0(x, y)$ can be exceedingly difficult. Furthermore, for the cascade problem values of $v(x, y)$ for all y are necessary, and hence, inversions valid for large or small values of y alone are insufficient. For this reason we have sought channel shapes which incorporate the contraction effect and yet are simple enough to carry out the subsequent manipulations. A very convenient choice turns out to consist of two parallel sections separated by a portion of an exponential channel as seen in Fig. 6. Mathematically this shape is expressed as

$$\left(\frac{h'}{h}\right) = -\alpha\,[H_0(x + b) - H_0(x - a)]$$

where $H_0(x)$ is the unit step function, i.e., equal to unity if the argument exceeds zero and equal to zero otherwise. The shape of the channel is indicated in Fig. 6.

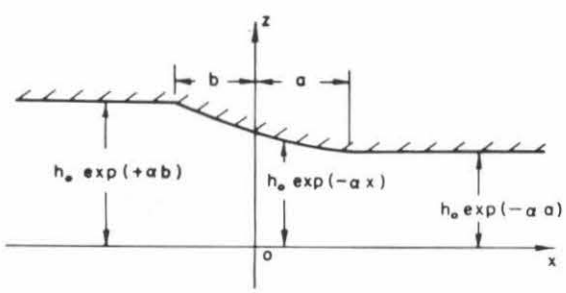

Fig. 6 Channel shape for central contraction

Equation (15) can now be solved for $p(x, k)$ in a straightforward way. However, the problem of inverting the extremely complicated function of k that p turns out to be was insurmountable and an alternative approach suggested in [4] was used.

This method consists of writing the differential equation for p in the form of an integral equation. Approximate solutions of the integral equation can then be obtained by iteration. These solutions again provide only $p(x, k)$ but it turns out that the first iteration can readily be inverted. For reference we reproduce the integral here: First we put

$$\left.\begin{aligned} p &= A(k)p_1(x, k), \qquad x > 0 \\ p &= B(k)p_2(x, k), \qquad x < 0 \end{aligned}\right\} \tag{17}$$

and then require that

$$\left.\begin{aligned} p_1 &\sim \exp(-kx) \quad \text{as} \quad x \to \infty \\ p_2 &\sim \exp(kx) \quad \text{as} \quad x \to -\infty \end{aligned}\right\} \tag{18}$$

Then p_1, p_2 satisfy [4]

$$p_1(x, k) = e^{-kx}\left[1 + \int_x^{\infty} \left(\frac{1 - e^{-2k(q-x)}}{2k}\right) g(q) e^{kq} p_1(q, k) dq\right]$$

and

$$p_2(x, k) = e^{kx}\left[1 + \int_{-\infty}^{x} \left(\frac{1 - e^{2k(q-x)}}{2k}\right) g(q) e^{-kq} p_2(q, k) dq\right] \tag{19}$$

In the above k stands for $|k|$. The $A(k)$ and $B(k)$ are found from equation (16) after the first iteration of equation (19) is carried out.

Only the first iteration of equation (19) was used in the present work. These turn out to be proportional to parameter α of Fig. 6. The second iteration, proportional to α^2, like the exact solution to equation (15), could not be exactly inverted to obtain u and v. Nevertheless, knowledge of the exact values of $p(x, k)$ did permit an accurate estimate to be made of the first iteration. This was done for a number of cascade cases computed. It was found that the approximate solution of equation (19) was systematically greater than the exact one, but that the difference decreased with increasing k and was in no case greater than about 0.4 percent for the numerical work that will be discussed later.

The above discussion sketches out how the velocity components for vortices and sources in the sectionally exponential channel of Fig. 6 can be obtained. These were carried out for isolated singularities for situations in which the singularity is located both within the region of contraction and exterior to the contraction (either up- or downstream) and they are summarized in Appendix 1. These same solutions are summed over the blades of the infinite cascade to obtain the kernel functions required in equation (11), and they are presented for reference in Appendix 2.

The convergence parameter α is presumed to be small and often, in such a case, a perturbation expansion scheme is used to obtain solutions of equation (7) as follows: Assume

$$\phi = \phi_0 + \alpha\phi_1 + \alpha^2\phi_2 \ldots .$$

The first term ϕ_0 corresponds to plane flow which has its solution for a line source, $\phi_0 = \frac{1}{2\pi} \ln(\sqrt{x^2 + y^2})$. Application of the expansion to equation (7) then gives

$$\Delta\phi_1 = -\frac{x}{2\pi(x^2 + y^2)}$$

a Poisson equation, to be satisfied by ϕ_1. This equation is readily solved and it is found that the first order addition to the velocity field is precisely that obtained by the technique of Fourier transforms just described. (Such an expansion procedure

will not, however, work for the fully exponential channel.) In retrospect it may be remarked that the main advantage in using transforms appears to be that in the transform method, the problem can be formulated and solved exactly so that numerical evaluations of the expansion procedure are possible. It is desirable to have such an estimate because, in the present case, for fixed α, the first order calculation in ϕ will be increasingly inaccurate as a and b become large, as then the channel of Fig. 6 can be less and less regarded as a perturbation from a channel of constant height.

Comparison with Previous Works

Two recent papers, references [5] and [6] have used a surface distribution of sources in the mean plane ($z = 0$) to achieve the effect of varying axial velocity component of freestream velocity. This undoubtedly alters V_{mn} and V_{mt} from the two-dimensional value in equation (11). The velocity fields of the singularity distributions were, however, still calculated on a two-dimensional basis. For an isolated airfoil, e.g., $K_{vn}(x, \xi)$ would then simply be $\left(\frac{1}{x - \xi}\right)$.

The present approach takes note of the fact that the flow fields of the singularities themselves are subject to the same limitation as the freestream velocity, namely that they take place in a channel of varying height. In both equations (5) and (6), the increase in axial velocity for positive stagger leads to a decrease of total circulation as compared to a two-dimensional calculation with constant axial velocity. It will be shown that when the departure from two-dimensionality is taken into account in the computation of the flow fields of the sources and vortexes, there is a further reduction of circulation. The reduction of circulation due to this latter consideration is at least as great as that due to variation of freestream velocity. Hence the incorporation of such an additional detail is not merely of academic interest. The formulation itself is in more general terms and enables a wider class of problems to be solved than merely that of cascade performance with varying axial velocity. For example, one could estimate the effect of contractions fully upstream or fully downstream of the airfoil chord, as will, in fact, be done.

Solution of the Integral Equation

With the channel geometry and mean angle of attack δ given, V_{mt} and V_{mn} in equation (11) are then known, and from Appendix 2, the kernel functions also. It only remains to solve the integral equation (11), to determine $\gamma(x)$, and from that the other characteristics of the cascade. The integral equation was solved by methods outlined in [7] and for reference the procedures adopted for the present problem are outlined in Appendix 3.

Discussion of Results

A number of examples including isolated airfoils and airfoils in cascade have been worked out. In all these, attention has been focused on the change in circulation about the airfoils caused by the contraction effect. In the following figures, this is given as the ratio of the quasi two-dimensional circulation ($\Gamma_{Q.T.D.}$) to the two-dimensional circulation ($\Gamma_{T.D.}$). To carry out the computations the value of the contraction parameter, α, was set equal to 0.1 and the mean angle of attack of the airfoil was put at 15 deg. The contraction effect is linear in α, however, so that the above ratio of the two circulations can be scaled to other values of α. The worked examples include flat plate cascades, circular arc cascades, and cascades with thickness. In the latter examples, the thickness distribution was that of symmetrical Joukowski airfoils.

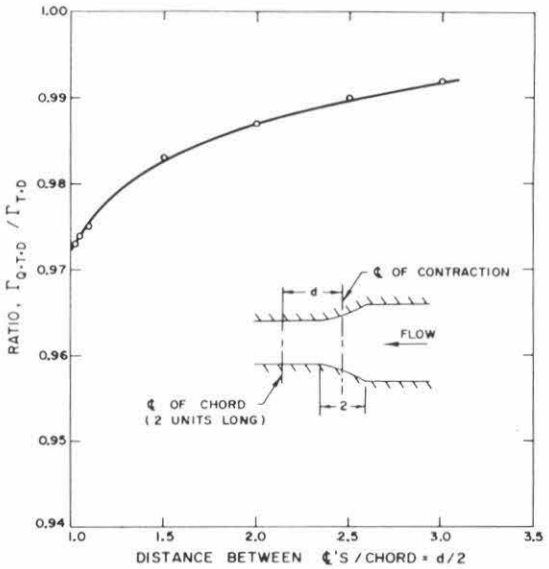

Fig. 7 Variation of circulation with distance of an upstream contraction from an isolated flat plate airfoil; stagger = 0 deg, α = 0.1, height ratio = 0.819

The principal results are given in Figs. 7–13. In Figs. 7–9, the effect of up- and downstream contractions on an otherwise plane cascade is shown for the circulation of an isolated flat plate. The first two graphs show the effect of an 18 percent contraction on an airfoil located at various distances away from the contraction. The effect, though small, could amount to a few percent in some applications. In Fig. 9, one end of the airfoil touches the contraction but the length of the contraction region varies, thus varying, with a fixed α of 0.1, the channel height ratio up to a maximum of 1.82. Again the effects are modest but noticeable. The remaining examples treated all have the airfoil within the contracting region. In these, one of the principal variables is the extent of the region of contraction, denoted by E. In all cases it was greater than the axial projection of blade chord.

A typical result for a compressor cascade in a contracting chan-

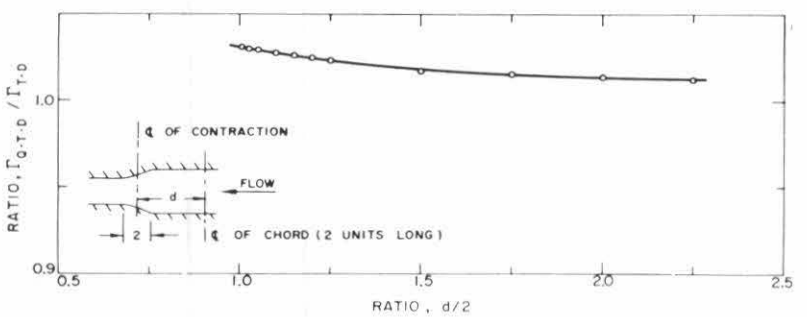

Fig. 8 Variation of circulation with distance of a downstream contraction from an isolated flat plate airfoil; stagger = 0 deg, α = 0.1

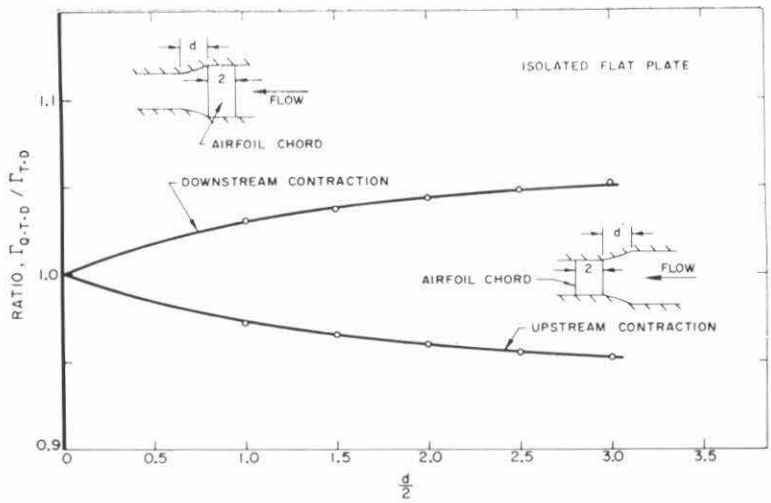

Fig. 9 Variation of circulation with extent of up- and downstream contractions for an isolated flat plate airfoil; stagger = 0 deg, α = 0.1

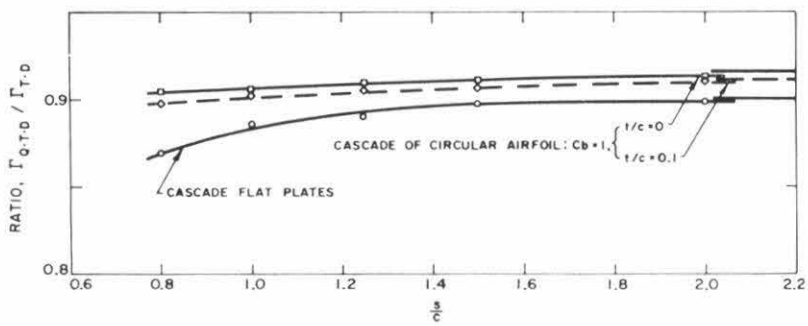

Fig. 10 Variation of circulation with solidity; α = 0.1, stagger = 45 deg, extent of contraction/axial projection of chord ratio = 1.06, mean angle of attack at center of chord = 15 deg, Cb = lift coefficient of the isolated airfoil at zero angle of attack

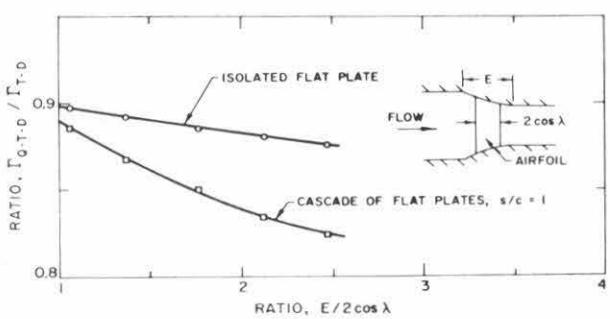

Fig. 11 Variation of circulation with extent of contraction; α = 0.1, stagger = 45 deg, contractions fully cover the plates, mean angle of attack at center of chord = 15 deg

nel is shown in Fig. 10. There, while there are some differences with thickness and camber, the effect of contraction is to reduce the circulation below its two-dimensional value by about 10 percent. For comparison, the channel contraction ratio is 0.87. The extent of contraction also has an effect on the airfoil circulation even if the contraction across the cascade itself remains constant as shown in Fig. 11. This effect is more noticeable in a cascade than for an isolated airfoil but depends somewhat upon airfoil geometry (Fig. 12). The effect of stagger angle is shown in Fig. 13, where it is seen that a minimum appears. In these cases, the speed-up of the axial velocity across the cascade is about 15 percent or so; there is a somewhat lesser reduction in circulation, but still it is of sufficient magnitude to be important in a technical application.

The flow angle leaving the cascade is of more direct interest in application. Two effects contribute to changing the flow direction through cascades with axial contraction, the circulation about the blades and the speed-up of axial velocity. The latter effect tends to make the leaving velocity vector more axial, and thus it increases the flow turning for a compressor cascade. On the other hand the general reduction of circulation caused by the channel contraction tends to offset this effect, suggesting that the leaving flow angle may be relatively unchanged from its two-dimensional value.

The leaving angle is conveniently expressed as the deviation from the airfoil exit camber angle. Calculations of the deviation angle, flow turning and inlet incidence angle were carried out for a circular arc cascade in both two-dimensional and quasi two-dimensional flow. The channel contraction resulted in a 13 percent increase in axial velocity across the cascade. These results are tabulated in Table 1. There it is seen that for the larger angle of attack and higher solidities the effect of channel contraction is to increase the deviation by about two deg or less. These comparisons are not made at the same inlet incidence angle, however, although the effect of incidence should be slight at the highest solidity. A similar result was found for cascades of flat plate airfoils where for stagger angles ranging from −30 to 60 deg and solidity of 0.5 to 1.25, channel contraction of the above amount caused only a slight change in deviation, being greater for the higher solidities and lesser than the corresponding two-dimensional value for the lower solidities.

The reduction in circulation is somewhat greater for purely cambered blades as is seen from Table 1. Then, the deviation angle departs only slightly from the two-dimensional value and it

is generally less except at the highest solidity than for the equivalent plane flow. It should be mentioned that the entering and leaving angles for the quasi two-dimensional case were computed at the entrance and exit to the blade row.

In a recent experimental study [8] on the effects of channel contraction on performance of cascades, it is proposed that the increase in axial velocity reduces the deviation angle linearly with the axial velocity ratio across the cascade section. The present calculations do indicate a similar linear dependence upon the axial velocity ratio; however, as the results of Table 1 show, there is not always a decrease in deviation angle. In fact, the change in deviation angle seems to depend upon all the parameters of the cascade and flow geometry. It does appear that the change in deviation angle is relatively modest in the examples tabulated in Table 1 and that the more important change is in the circulation about the blades.

A computing program has been developed to carry out the calculations in the present work. It is available in the form of a report [9].

Acknowledgments

This research was accomplished with the support of the Office of Naval Research under Contract Nonr 220(59). The assistance of Mrs. Z. Harrison in the numerical calculations is gratefully acknowledged.

References

1 Mani, R., "Quasi Two-Dimensional Flows Through Cascades," PhD thesis, California Institute of Technology, 1967.

2 Mellor, G. L., "An Analysis of Axial Compressor Cascade Aerodynamics," *Journal of Basic Engineering*, TRANS. ASME, Series D, Vol. 81 No. 3, Sept. 1959, pp. 362–378.

3 Hawthorne, W. R., "Induced Deflection Angle in Cascades," *Journal of the Aeronautical Sciences*, Vol. 16, No. 4, 1949, p. 252.

4 Lighthill, M. J., "The Fundamental Solution for Small Steady Three-Dimensional Disturbances of a Two-Dimensional Parallel Shear Flow," *Journal of Fluid Mechanics*, Vol. 3, 1957, p. 113.

5 Kubota, S., "Cascade Performance with Accelerated or Decelerated Axial Velocity," *Bulletin of the Japan Society of Mechanical Engineers*, Vol. 5, No. 19, 1962, p. 450.

6 Pollard, D., and Horlock, J. H., "A Theoretical Investigation of the Effect of Change in Axial Velocity on the Potential Flow Through a Cascade of Airfoils," ARC CP No. 619, 1963.

7 Muskhelishvili, N. I., *Singular Integral Equations*, P. Noordhoff N. V., Groningen, Holland, 1953.

8 Pollard, D., and Gostelow, J. P., "Some Experiments at Low Speed on Compressor Cascades," JOURNAL OF ENGINEERING FOR POWER, TRANS. ASME, Series A, Vol. 89, No. 3, July 1967, pp. 427–436.

9 Mani, R., "A Method of Calculating Quasi Two-Dimensional Flows Through Cascades," California Institute of Technology Engineering Report No. E-79.10 (in preparation).

10 *Handbook of Mathematical Functions with Formulas, Graphs and Mathematical Tables*, Abramowitz, M., and Stegun, I. A., eds., National Bureau of Standards, 1964

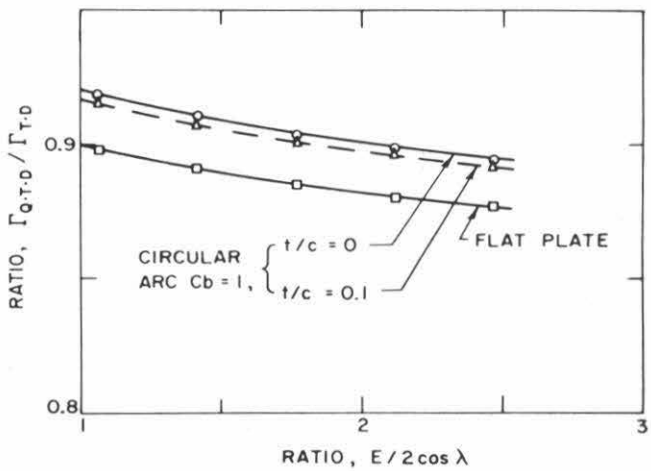

Fig. 12 Variation of circulation with extent of contraction for three types of isolated airfoils; α = 0.1, stagger = 45 deg, Cb = lift coefficient of the isolated airfoil at zero angle of attack, contractions fully cover the airfoils

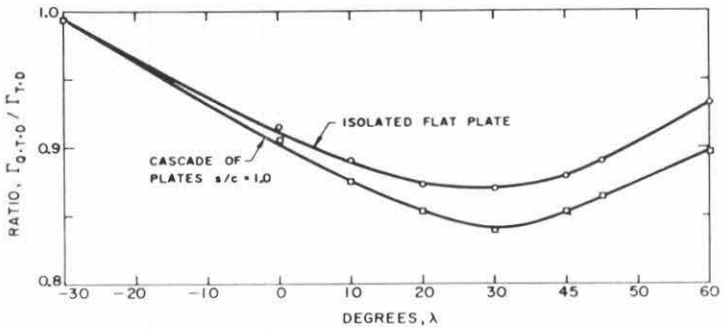

Fig. 13 Variation of circulation with stagger; α = 0.1, extent of contraction = 2.05, chord length = 2, mean angle of attack at center of chord = 15 deg

Table 1 Characteristics of circular arc cascades in two-dimensional and quasi two-dimensional flow

Cb = 1.00, Stagger Angle = 45 deg, Contraction of Cascade = 0.87, $Q.T.D.$ = quasi two-dimensional

Solidity	Inlet incidence angle $Q.T.D.$ deg	Inlet incidence angle $T.D.$ deg	Flow turning angle $Q.T.D.$ deg	Flow turning angle $T.D.$ deg	Deviation angle $Q.T.D.$	Deviation angle $T.D.$	$\Gamma_{Q.T.D}/\Gamma_{T.D.}$	Angle of attack at center of chord
1.25	7.01	6.35	34.84	36.07	9.96	8.08	0.905	15 deg
1.00	6.56	5.85	32.18	32.78	12.19	10.88	0.907	15 deg
0.80	5.90	5.11	28.57	28.39	15.13	14.52	0.910	15 deg
0.67	5.22	4.34	25.28	24.46	17.74	17.68	0.912	15 deg
0.50	4.02	3.01	20.32	18.69	21.51	21.11	0.915	15 deg
0.00							0.916	15 deg
1.25	−9.74	−10.69	20.48	19.68	7.58	7.43	0.848	0 deg
1.00	−10.48	−11.53	18.48	17.27	8.83	9.00	0.850	0 deg
0.80	−11.30	−12.47	16.37	14.70	10.13	10.62	0.846	0 deg
0.67	−11.98	−13.26	14.69	12.66	11.14	11.87	0.848	0 deg
0.50	−12.97	−14.42	12.31	9.79	12.52	13.58	0.850	0 deg
0.00							0.858	0 deg

APPENDIX 1

Fundamental Solutions For Isolated Singularities

For the channel of Fig. 6 with subscripts s and v denoting "source" and vortex" respectively and for $-b \leq x \leq a$, the velocity components for a unit strength of singularity are

$$u_s = \frac{1}{2\pi}\left[\frac{x}{x^2+y^2} + \frac{\alpha x^2}{2(x^2+y^2)} - \frac{\alpha}{8}\ln\left\{\frac{((2a-x)^2+y^2)((x+2b)^2+y^2)}{(x^2+y^2)^2}\right\}\right]$$

$$v_s = \frac{1}{2\pi}\left[\frac{y}{x^2+y^2} - \frac{\alpha}{4}\left[\tan^{-1}\left(\frac{x+2b}{y}\right) - \tan^{-1}\left(\frac{2a-x}{y}\right)\right] + \frac{\alpha xy}{2(x^2+y^2)}\right] \quad \text{to} \quad 0(\alpha),$$

and

$$u_v = -\frac{1}{2\pi}\left[\frac{y}{x^2+y^2} + \frac{\alpha xy}{2(x^2+y^2)} + \frac{\alpha}{4}\left\{\tan^{-1}\left(\frac{x+2b}{y}\right) - \tan^{-1}\left(\frac{2a-x}{y}\right)\right\}\right]$$

$$v_v = \frac{1}{2\pi}\left[\frac{x}{x^2+y^2} + \frac{\alpha x^2}{2(x^2+y^2)} + \frac{\alpha}{8}\ln\left[\frac{((x+2b)^2+y^2)((2a-x)^2+y^2)}{(x^2+y^2)^2}\right]\right].$$

For a fully upstream contraction for which

$$h = h_0 \exp\,[\alpha(b-a)] \qquad \text{for } x \leq -b$$
$$h = h_0 \exp\,[-\alpha(x-b)] \qquad \text{for } -b \leq x \leq -a$$

and

$$h = h_0 \qquad \text{for } -a \leq x,$$

the solutions are

$$u_s = \frac{1}{2\pi}\left[\frac{x}{x^2+y^2} - \frac{\alpha}{8}\ln\left[\frac{(x+2b)^2+y^2}{(x+2a)^2+y^2}\right]\right]$$

$$v_s = \frac{1}{2\pi}\left[\frac{y}{x^2+y^2} - \frac{\alpha}{4}\left[\tan^{-1}\left(\frac{y}{x+2a}\right) - \tan^{-1}\left(\frac{y}{x+2b}\right)\right]\right]$$

$$u_v = \frac{1}{2\pi}\left[\frac{y}{x^2+y^2} + \frac{\alpha}{4}\left\{\tan^{-1}\left(\frac{y}{x+2a}\right) - \tan^{-1}\left(\frac{y}{x+2b}\right)\right\}\right]$$

$$v_v = \frac{1}{2\pi}\left[\frac{x}{x^2+y^2} + \frac{\alpha}{8}\ln\left[\frac{(x+2b)^2+y^2}{(x+2a)^2+y^2}\right]\right]$$

For a fully downstream contraction for which

$$h = h_0 \qquad \text{for } x \leq a$$
$$h = h_0 \exp\,[\alpha(x-a)] \qquad \text{for } a \leq x \leq b$$

and

$$h = h_0 \exp\,[\alpha(b-a)] \qquad \text{for } b \leq x,$$

the solutions are

$$u_s = \frac{1}{2\pi}\left[\frac{x}{x^2+y^2} + \frac{\alpha}{8}\ln\left[\frac{(2b-x)^2+y^2}{(2a-x)^2+y^2}\right]\right]$$

$$v_s = \frac{1}{2\pi}\left[\frac{y}{x^2+y^2} - \frac{\alpha}{4}\left[\tan^{-1}\left(\frac{y}{2a-x}\right) - \tan^{-1}\left(\frac{y}{2b-x}\right)\right]\right]$$

$$u_v = -\frac{1}{2\pi}\left[\frac{y}{x^2+y^2} + \frac{\alpha}{4}\left[\tan^{-1}\left(\frac{y}{2a-x}\right) - \tan^{-1}\left(\frac{y}{2b-x}\right)\right]\right]$$

$$v_v = \frac{1}{2\pi}\left[\frac{x}{x^2+y^2} - \frac{\alpha}{8}\ln\left[\frac{(2b-x)^2+y^2}{(2a-x)^2+y^2}\right]\right]$$

APPENDIX 2

Fundamental Singular Solutions in a Cascade

Consider the case of a contraction that fully covers the chords. The chords are taken as two units long. The axis of convergence is along the cascade axis and the convergence is located so that the centerline of the convergence and that of the chords coincide. The extent of the contraction is E so that $[E \div 2\cos(\lambda)]$ is the fraction of the chords covered by the contraction. Since the contraction is assumed to fully cover the chord, $[E \div 2\cos(\lambda)]$ is always greater than unity.

The fundamental solutions in Appendix 1 are in terms of an x-y coordinate system with the x-axis along the axis of convergence. In evaluating the contribution to $K_{vnc}(x, \xi)$, for example, from a unit vortex located at S_n in Fig. 5, one uses the fundamental solutions of Appendix 1 with an x'-y' coordinate system as shown in Fig. 5.

In terms of x, ξ

$$x' = (x-\xi)\cos(\lambda)$$
$$y' = -ns + (x-\xi)\sin(\lambda)$$
$$a = \frac{E}{2} - \xi\cos(\lambda), \qquad b = \frac{E}{2} + \xi\cos(\lambda)$$

With these values of x', y', a, b one determines u', v' which are velocities parallel to the x' and y'-axes at P due to the unit vortex at S_n.

$$u' = -\frac{1}{2\pi}\left[\left(1 + \frac{\alpha}{2}(x-\xi)\cos\lambda\right) \times \left[\frac{(x-\xi)\sin(\lambda) - ns}{(x-\xi)^2 + n^2s^2 - 2ns(x-\xi)\sin(\lambda)}\right] + \frac{\alpha}{4}\left\{\tan^{-1}\left[\frac{E-(x+\xi)\cos\lambda}{ns-(x-\xi)\sin\lambda}\right] - \tan^{-1}\left[\frac{E+(x+\xi)\cos\lambda}{ns-(x-\xi)\sin\lambda}\right]\right\}\right]$$

$$v' = \frac{1}{2\pi}\left[\left(1 + \frac{\alpha}{2}(x-\xi)\cos\lambda\right) \times \left[\frac{(x-\xi)\cos\lambda}{(x-\xi)^2 + n^2s^2 - 2ns(x-\xi)\sin\lambda}\right] + \frac{\alpha}{8}\ln\{[((x+\xi)\cos\lambda + E)^2 + n^2s^2 - 2ns(x-\xi)\sin\lambda + (x-\xi)^2\sin^2\lambda]\,[(E-(x+\xi))^2 + n^2s^2 - 2ns(x-\xi)\sin\lambda + (x-\xi)^2\sin^2\lambda] \div [(x-\xi)^2 + n^2s^2 - 2ns(x-\xi)\sin\lambda]^2\}\right]$$

The velocity normal to the chord at P due to the unit vortex at S_n is

$$v = -u'\sin(\lambda) + v'\cos(\lambda).$$

$K_{vnca}(x, \xi)$ will consist of an infinite sum of such contributions

from unit vortexes at $S_{-\infty}, \ldots S_{-1}, S_0, S_1, \ldots S_\infty$.

The first portion of $K_{vnca}(x, \xi)$ is

$$\sum_{n=-\infty}^{n=\infty} \left\{ \frac{(x-\xi) = ns \sin(\lambda)}{(x-\xi)^2 - 2ns(x-\xi)\sin(\lambda) + n^2s^2} \right\} \times \left(1 + \frac{\alpha}{2}(x-\xi)\cos(\lambda)\right).$$

This portion is summable in closed form and the sum is (see Appendix 1 of [2]):

$$\left(1 + \frac{\alpha}{2}(x-\xi)\cos\lambda\right)\left[\frac{\cos\lambda \sin h\left(\frac{2\pi}{s}(x-\xi)\cos\lambda\right) + \sin\lambda \sin\left(\frac{2\pi}{s}\sin\lambda(x-\xi)\right)}{\cos h\left(\frac{2\pi}{s}\cos\lambda(x-\xi)\right) - \cos\left(\frac{2\pi}{\lambda}(x-\xi)\sin\lambda\right)}\right]$$

The remaining part of K_{vnca} is:

$$\sum_{-\infty}^{\infty} \left\{ \frac{\alpha \sin(\lambda)}{4} \left\{ \tan^{-1}\left(\frac{E - (x+\xi)\cos(\lambda)}{ns - (x-\xi)\sin(\lambda)}\right) - \tan^{-1}\left(\frac{E + (x+\xi)\cos(\lambda)}{ns - (x-\xi)\sin(\lambda)}\right)\right\} + \frac{\alpha\cos(\lambda)}{8} \ln\left[\frac{(((x+\xi)\cos(\lambda) + E)^2 + y'^2)((E - (x+\xi)\cos(\lambda))^2 + y'^2)}{((x-\xi)^2 + n^2s^2 - 2ns(x-\xi)\sin(\lambda))^2}\right]\right\}$$

where $y' = -ns + (x-\xi)\sin(\lambda)$.

The above sum is taken exactly with n from $-r$ to $+r$. The term r designates an integer large enough so that $\frac{E}{rs}$, $\frac{(x-\xi)}{rs}$, and $\left(\frac{x+\xi}{rs}\right)$ are quite small. The remainder of the sum is found by expanding the above expressions in a Taylor series for large (ns) and retaining the leading terms. The result for the remainder of the sum is, approximately:

$$\left[\frac{\alpha\sin\lambda}{4}\left\{-\frac{2\sin(2\lambda)}{s^2}(x^2 - \xi^2)\right\} + \frac{\alpha\cos\lambda}{8}\left\{\frac{4}{s^2}(E^2 + 4x\xi\cos^2\lambda)\right\}\right]\left[\frac{1}{r+1} + \frac{1}{2(r+1)^2}\right]$$

reference [10]

APPENDIX 3

Solution of the Integral Equation

Equation (11) governing the distribution of vorticity can be expressed in the form

$$\frac{1}{2\pi}\int_{-1}^{1} \gamma(\xi)K_v(x, \xi)d\xi = f(x) \qquad (20)$$

where $-1 < x < 1$ and the most singular term of $K_v(x, \xi)$ is $\frac{1}{(x-\xi)}$. We follow in the subsequent treatment methods based on [7].

The formal steps needed to solve equation (20) are as follows:

1 Let $x = \cos(\theta)$, $\xi = \cos(\phi)$ so that as x, ξ run from -1 to 1, θ and ϕ run from π to 0. Let

$$K_x(x, \xi) = \frac{1}{(x-\xi)} + K_{vr}(x, \xi)$$

2 Assume for $\gamma(\cos\theta)$ the usual airfoil type series with the square root singularity at the leading edge and with all terms vanishing at the trailing edge (due to the Kutta Joukowski condition):

$$\gamma(\cos(\theta)) = a_0 \tan\left(\frac{\theta}{2}\right) + \sum_{n=1}^{N} a_n \sin(n\theta)$$

The N to be used above will be discussed later.

3 Compute $(N+1)(N+2)$ coefficients in the double Fourier series expansion of $K_{vr}(x, \xi)$, i.e.,

$$K_{vr}(x, \xi) = \sum_{0}^{\infty}\sum_{0}^{\infty} b_{lm} \cos(l\theta)\cos(m\phi)$$

compute $b_{00}, b_{01}, \ldots b_{N,N+1}$.

4 Compute the first $(N+1)$ coefficients, i.e, $d_0, \ldots d_N$ in the Fourier analysis of

$$2f(x) = d_0 + \sum_{1}^{\infty} d_n \cos(n\theta)$$

5 The $a_0, \ldots a_N$ may be found by solving the set of simultaneous equations:

$$a_0\left(\delta_{r0} + b_{r0} - \frac{b_{r1}}{2}\right) + a_1\left(\frac{b_{r0}}{2} - \frac{b_{r2}}{4} + \delta_{r1}\right) + \sum_{2}^{N} a_n\left(\delta_{nr} + \frac{1}{4}(b_{r,n-1} - b_{r,n+1})\right) = d_r.$$

With $r = 0, 1, \ldots N$, δ_{mn} is the Kronecker delta function, equal to zero if $m \neq n$, and equal to one if $m = n$.

With regard to the N, we select arbitrarily some N, carry out the solution of the set of simultaneous equations, and then check whether the decay of the last a_n's is rapid enough for the chosen N. Even for complicated cascade geometries, the use of $N = 4$, i.e., using a 5-term description of the vorticity series, seems satisfactory (i.e., rapid decay of the last few a_n's is observable). The integrated total circulation equals $\pi\left(a_0 + \frac{a_1}{2}\right)$ and depends only on the first two terms of the vorticity series. For chosen N, one has to compute $(N+1)$ coefficients in the d-series and $(N+1)(N+2)$ coefficients in the b-series, and so the labor of computation increases rather steeply with increase of N.

There is one analytical difficulty associated with $K_{vr}(x, \xi)$. For all cases where the contraction fully covers the airfoils $K_{vr}(x, \xi)$ has a weak logarithmic singularity behaving like $\ln(|x-\xi|)$. The rest of $K_{vr}(x, \xi)$ is continuous and can be directly fed into the computer for double Fourier analysis. The double Fourier analysis of $\ln|x-\xi|$ can be got by using Cauchy principal values. This expansion is, of course, not convergent along $x = \xi$. It is:

$$\ln|x-\xi| = -\ln(2) - 2\sum_{1}^{\infty} \frac{\cos(n\theta)\cos(n\phi)}{n}$$

for $x \neq \xi$ and $\theta \neq \phi$.

The b_{lm} matrix associated with $\ln|x-\xi|$ can be added on separately to the double Fourier analysis of the continuous portion of $K_{vr}(x, \xi)$.

Printed in U. S. A.